wjert, 2025, Vol. 11, Issue 3, 251-267. Review Article ISSN 2454-695X

World Journal of Engineering Research and Technology
WJERT
www.wjert.org SJIF Impact Factor: 7.029

NUMERICAL STUDY OF CONVECTIVE MHD FLOW OF A TERNARY NANOFLUID OVER A STRETCHING SHEET WITH VISCOUS AND JOULE HEATING EFFECTS

Janapati Siva Shankar Rao*

Lecturer in Mathematics, Government College (Autonomous), Anantapur-515003, A. P., India.

Article Received on 23/01/2025 **Article Revised on 13/02/2025** **Article Accepted on 03/03/2025**

***Corresponding Author**
Dr. Janapati Siva Shankar Rao
Lecturer in Mathematics, Government College (Autonomous), Anantapur-515003, A. P., India.

ABSTRACT

This paper investigates the steady, two-dimensional convective magneto hydrodynamic (MHD) boundary layer flow of a ternary ($Cu - Fe_3O_4 - SiO_2/H_2O$) and hybrid nanofluids ($Cu - Fe_3O_4/H_2O$) over a convectively heated elastic sheet. The governing equations with convective boundary conditions are solved numerically using a mathematical software tool, employing the RKF-45 method along with the shooting technique. The plots of velocity and temperature profiles for both $Cu - Fe_3O_4 - SiO_2/H_2O$ and $Cu - Fe_3O_4/H_2O$ for various parameters are captured. The Grashof number (G) enhances velocity and depreciates temperature in both nanofluids. It is noticed that higher dissipative energy (E_c) larger the velocity and temperature in the entire flow region. Skin friction (τ) increases and Nusselt number (Nu) decreases at the stretching sheet in both ternary as well as hybrid nanofluid with the increasing values of $\Phi / R_d / E_c / Q_s$. This paper endorses that ternary nanofluid has an excellent thermal accomplishment over the hybrid nanofluid.

KEYWORDS: Ternary nanofluid, hybrid nanofluid, convective boundary conditions, skin friction, Nusselt number.

1. INTRODUCTION

Nanoparticle research has gained considerable attention due to its potential applications in fields such as medicine, optics, and electronics. The study of squeezing flow between parallel boundaries has intrigued many researchers and engineers because of its relevance to various engineering processes, metal fluid purification, and industries like food and chemicals. This phenomenon also finds applications in shaping and squeezing operations. Nanofluids, which consist of solid particles ranging from 1 to 100 nanometers dispersed in base fluids, have shown promise in enhancing the thermal conductivity and heat transfer properties of the base fluids (as noted by Choi and Eastman[1] and Buongiorno.[2]) Further research by Eastman et al.[3] demonstrated the measurement of thermal conductivity in $Cu/C_2H_6O_2$ nanofluids. Sheikholeslami and Ganji[4] explored the impact of particle shape on forced convective flow of nanofluids in the presence of Lorentz forces. Additionally, several studies have investigated the behaviour of nanofluids under varying conditions, as discussed in references such as Yin et al.[5] and Zhang et al.[6]

A few years later, researchers identified that combining multiple nanosized particles in a clear base fluid enhances its thermal properties, leading to the development of what are now called "hybrid nanofluids." These fluids are particularly effective in cooling high-temperature thermal systems and are widely used in applications such as solar energy systems, heat exchangers, generator cooling, transformers, heat pipes, and nuclear technology. Experimental studies by Jana et al.[7] brought further insights into hybrid nanofluids. It was observed that the heat conduction efficiency of these fluids improves significantly with an increased volume fraction of nanoparticles, a phenomenon earlier reported by Suresh et al.[8] Other researchers have also explored the potential of hybrid nanofluids, as noted in studies.[9–17] For instance, Satya Narayana et al.[18] investigated the flow of $Cu\text{-}Al_2O_3/H_2O$ hybrid nanofluids over a porous, stretching sheet under the influence of temperature-dependent viscosity and viscous dissipation. Their findings showed that the velocity profile of hybrid nanofluids improves with a higher convection parameter. Furthermore, due to variable viscosity, hybrid nanofluids achieve faster boundary convergence compared to Al_2O_3/H_2O nanofluids. Extensive research on hybrid nanoparticle mixtures, their applications, and developments can be found in references.[19–20]

In recent years, researchers have combined three distinct types of nanoparticles within a base fluid to create a new class of nanofluids known as "ternary hybrid nanofluids." This

innovative development emerged due to the growing industrial demand for advanced cooling solutions with superior thermal properties. To address these requirements, a trihybrid nanofluid was introduced, offering enhanced thermal characteristics. Mousavi et al.[21] explored the behaviour of a trihybrid nanofluid composed of TiO_2, CuO, and MgO suspended in water. Sahoo et al.[22] proposed a novel correlation aimed at improving the viscosity of such fluids. Further interest in ternary hybrid nanofluids has been spurred by recent investigations.[23–27] Jafar Hasnain et al.[28] examined the thermal behaviour of water- and engine oil-based ternary nanofluids containing nanoparticles of various shapes over both linear and nonlinear stretching sheets. Their findings indicated that increasing the nanoparticle volume fraction led to higher temperatures in ternary nanofluids compared to hybrid nanofluids, for both linear and nonlinear stretching scenarios. Adnan and Ashraf[29] investigated the influence of a magnetic field on trihybrid nanofluid flow under convective heating conditions, comparing the results with hybrid nanofluid flow. The advancements in trihybrid nanofluid research have drawn significant attention and continue to encourage further studies.[30–32]

Aly and Pop[33] analysed stagnation point flow and heat transfer characteristics of hybrid nanofluids, factoring in slip conditions and the effects of viscous dissipation. Their study included a stability analysis near the endpoint within a regime exhibiting dual solutions. Lund et al.[34] focused on the stability of copper-alumina/water hybrid nanofluids over a stretching or shrinking surface, also considering viscous dissipation. Using the three-stage Lobatto IIIa method, they identified two solutions, determining that the first is stable while the second lacks stability. Afridi et al.[35] explored thermal behaviour in the boundary layer flows described by Blasius and Sakiadis for hybrid nanofluids. Their work included the study of two hybrid nanofluid types—Cu-Al_2O_3/water and Cu-Al_2O_3/kerosene oil—and reported that temperature rises in both systems.

The present study focuses on the analysis of convective MHD flow of ternary nanofluid ($Cu - Fe_3O_4 - SiO_2/H_2O$) over a stretching sheet accounting for viscous and joul heating dissipations. Here partial differential equations are solved numerically by employing RKF method with shooting scheme. Results so arrived are strongly cope up with the existing results. This paper also compares the effects of different parameters on ternary ($Cu - Fe_3O_4 - SiO_2/H_2O$) and hybrid $(Cu - Fe_3O_4/H_2O)$nanofluids.

2. Formulation of the problem

In this paper the steady, two-dimensional convective magneto hydrodynamic (MHD) boundary layer flow of a ternary nanofluid over a convectively heated elastic sheet is examined. The ternary nanofluid comprises copper (Cu) nanoparticles, iron oxide (Fe_3O_4), and silicon dioxide (SiO_2) dispersed in water as the base fluid. The schematic representation of the flow configuration is provided in Fig. (1). The X-axis is aligned with the flow direction, while the Y-axis is perpendicular to it. The velocity along the surface is defined as $U_w(x) = ax$, where a is a constant with dimensions of inverse time (t^{-1}). The surface temperature is T_w, and the ambient temperature is T_∞. A uniform transverse magnetic field of strength B_o is applied perpendicular to the X-axis. Incorporating viscous and Joule heating effects and conventional boundary conditions, the governing equations for the ternary nanofluid flow are derived as follows.

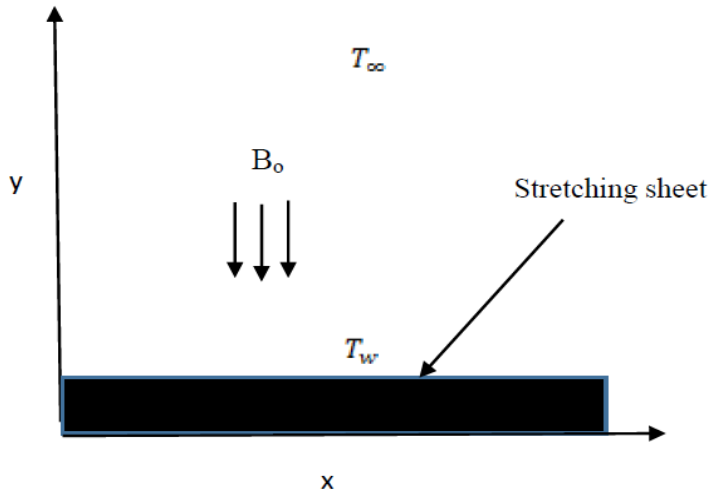

Fig. 1: Geometry of the flow configuration.

$$\frac{\partial u}{\partial x}+\frac{\partial v}{\partial y}=0 \tag{1}$$

$$u\frac{\partial u}{\partial x}+v\frac{\partial u}{\partial y}=\frac{\mu_{thnf}}{\rho_{thnf}}\frac{\partial^2 u}{\partial y^2}-\frac{\sigma_{thnf}}{\rho_{thnf}}B_0{}^2u+\frac{(\rho\beta)_{thnf}}{\rho_{thnf}}g(\mathrm{T}-\mathrm{T}_\infty) \tag{2}$$

$$(\rho c_p)_{thnf}\,v\frac{\partial T}{\partial y}=k_{thnf}\frac{\partial^2 T}{\partial y^2}+Q(\mathrm{T}-\mathrm{T}_\infty)-\frac{\partial q_r}{\partial y}+2\mu_{thnf}(\frac{\partial u}{\partial y})^2+(\sigma_{thnf}\,\mu_e{}^2\,\mathrm{H}_0{}^2)\,\mathrm{u}^2 \tag{3}$$

The appropriate boundary conditions are

$$\left.\begin{array}{l} u = ax, \mathrm{v} = 0\,,\ -k_{thnf}\dfrac{\partial T}{\partial y} = h_f(\mathrm{T}_w - \mathrm{T}) \text{ at } y = 0 \\ u \to 0,\ T \to T_\infty \text{ as } y \to \infty \end{array}\right\} \tag{4}$$

The radiative heat term q_r, based on the Roseland approximation, is expressed as follows

$$q_r = -\frac{4\sigma^*}{3k^*}\frac{\partial T^4}{\partial y} \tag{5}$$

The representation of T^4 around T_∞ using Taylor's series is expressed as

$$T^4 = 4T_\infty^3 T - 3T_\infty^4 \tag{6}$$

Then we have

$$\frac{\partial q_r}{\partial y} = \frac{-16\sigma^* T_\infty^3}{3k^*}\frac{\partial^2 T}{\partial y^2} \tag{7}$$

Table 1: Values of nanoparticles.

Nanofluid particles				**Base fluid**
Thermal & physical properties	Cu	Fe_3O_4	SiO_2	Water
C_p (j/kg K)	385	670	765	4179
ρ (kg m^3)	8933	5180	2270	997.1
k (W/m K)	400	9.7	1.4013	0.6071
βx10^{-5} (1/k)	1.67	0.5	0.056	21.0
σ(*s/m*)	5.96×10^7	2.5×10^{-4}	3.5×10^6	5.5×10^{-6}

Table 2: Properties of nanoparticles.

Thermal & physical properties	**Ternary, Hybrid & Mono nanofluids**
Viscosity (μ) **N.s / m^2**	$\mu_{thnf} = \dfrac{1}{\mu_f^{-1}(1-(\Phi_1+\Phi_2+\Phi_3))^{2.5}}$, $\mu_{hnf} = \dfrac{1}{\mu_f^{-1}(1-(\Phi_1+\Phi_2))^{2.5}}$, $\mu_{nf} = \dfrac{1}{\mu_f^{-1}(1-\Phi_1)^{2.5}}$
Density(ρ) Kg / m^3	$\rho_{thnf} = (1-(\Phi_1+\Phi_2+\Phi_3))\rho_f + \Phi_1\rho_{s1} + \Phi_2\rho_{s2} + \Phi_3\rho_{s3}$, $\rho_{hnf} = (1-(\Phi_1+\Phi_2))\rho_f + \Phi_1\rho_{s1} + \Phi_2\rho_{s2}$, $\rho_{nf} = (1-\Phi_1)\rho_f + \Phi_1\rho_{s1}$
Specific heat (C_p), J / k	$(\rho Cp)_{thnf} = (1-(\Phi_1+\Phi_2+\Phi_3))(\rho Cp)_f + \Phi_1(\rho Cp)_{s1} + \Phi_2(\rho Cp)_{s2} + \Phi_3(\rho Cp)_{s3}$ $(\rho Cp)_{hnf} = (1-(\Phi_1+\Phi_2))(\rho Cp)_f + \Phi_1(\rho Cp)_{s1} + \Phi_2(\rho Cp)_{s2}$

	$(\rho Cp)_{nf} = (1-\Phi_1)(\rho Cp)_f + \phi_1(\rho Cp)_{s1}$
Thermal expansion $(\rho\beta)$	$(\rho\beta)_{thnf} = (1-(\Phi_1+\Phi_2+\Phi_3))(\rho\beta)_f + \Phi_1(\rho\beta)_{s1} + \Phi_2(\rho\beta)_{s2} + \Phi_3(\rho\beta)_{s3}$ $(\rho\beta)_{hnf} = (1-(\Phi_1+\Phi_2))(\rho\beta)_f + \Phi_1(\rho\beta)_{s1} + \Phi_2(\rho\beta)_{s2}$ $(\rho\beta)_{nf} = (1-\Phi_1)(\rho\beta)_f + \Phi_1(\rho\beta)_{s1}$,
Thermal conductivity (k) W / m.k	$\frac{k_{thnf}}{k_{hnf}} = \frac{\Phi_1 k_{s1} + \Phi_2 k_{s2} + \Phi_3 k_{s3} + 2(\Phi_1+\Phi_2+\Phi_3)k_f + 2(\Phi_1+\Phi_2+\Phi_3)(\Phi_1 k_{s1} + \Phi_2 k_{s2} + \Phi_3 k_{s3}) - 2(\Phi_1+\Phi_2+\Phi_3)^2 k_f}{\Phi_1 k_{s1} + \Phi_2 k_{s2} + \Phi_3 k_{s3} + 2(\Phi_1+\Phi_2+\Phi_3)k_f - (\Phi_1+\Phi_2+\Phi_3)(\Phi_1 k_{s1} + \Phi_2 k_{s2} + \Phi_3 k_{s3}) + (\Phi_1+\Phi_2+\Phi_3)^2 k_f}$ $\frac{k_{hnf}}{k_{nf}} = \frac{\Phi_1 k_{s1} + \Phi_2 k_{s2} + 2(\Phi_1+\Phi_2)k_f + 2(\Phi_1+\Phi_2)(\Phi_1 k_{s1} + \Phi_2 k_{s2}) - 2(\Phi_1+\Phi_2)^2 k_f}{\Phi_1 k_{s1} + \Phi_2 k_{s2} + 2(\Phi_1+\Phi_2)k_f - (\Phi_1+\Phi_2)(\Phi_1 k_{s1} + \Phi_2 k_{s2}) + (\Phi_1+\Phi_2)^2 k_f}$ $\frac{k_{nf}}{k_f} = \frac{\Phi_1 k_{s1} + 2(\Phi_1)k_f + 2(\Phi_1)(\Phi_1 k_{s1}) - 2(\Phi_1)^2 k_f}{\Phi_1 k_{s1} + 2(\Phi_1)k_f - (\Phi_1)(\Phi_1 k_{s1}) + (\Phi_1)^2 k_f}$
Electrical conductivity (σ)	$\frac{\sigma_{thnf}}{\sigma_{hnf}} = \frac{\sigma_{s1}(1+2\Phi_1) + \sigma_{hnf}(1-2\Phi_1)}{\sigma_{s1}(1-\Phi_1) + \sigma_{hnf}(1+\Phi_1)}$, $\frac{\sigma_{hnf}}{\sigma_{nf}} = \frac{\sigma_{s2}(1+2\Phi_2) + \sigma_{nf}(1-2\Phi_2)}{\sigma_{s2}(1-\Phi_2) + \sigma_{nf}(1+\Phi_2)}$ $\frac{\sigma_{nf}}{\sigma_f} = \frac{\sigma_{s3}(1+2\Phi_3) + \sigma_f(1-2\Phi_3)}{\sigma_{s3}(1-\Phi_3) + \sigma_f(1+\Phi_3)}$

In the expressions provided Φ_1, Φ_2 and Φ_3 are solid volume fractions of Cu, Fe_3O_4 and SiO_2 respectively. The velocity and temperature profiles are obtained using the similarity transformations outlined below.

$$u = axf'(\Omega),\ v = -\sqrt{a\nu_f}\, f(\Omega),\ \Omega = \sqrt{\frac{a}{\nu_f}}y,\ \theta(\Omega) = (T - T_\infty)(T_w - T_0)^{-1} \tag{8}$$

The similarity variables defined in equation (8) fulfil the conditions of equation (1), ensuring they accurately describe the fluid flow. By substituting the similarity variables from equation (8) into equations (1) through (4) and utilizing the relationship in equation (7), the following system of equations is derived:

$$f_{\Omega\Omega\Omega} - (A_1A_2)[(f_\Omega)^2 - ff_{\Omega\Omega}] - A_1A_6M^2 f_\Omega + (A_1A_3G)\theta = 0 \tag{9}$$

$$A_1[A_5 + \frac{4}{3}R_d]\theta_{\Omega\Omega} + A_1A_4P_r f\theta_\Omega + A_1P_rQ_s\theta + E_cP_r(f_{\Omega\Omega})^2 + A_1A_6P_rM^2E_c(f_\Omega)^2 = 0 \tag{10}$$

Where $G = \frac{\beta_f g(T_w - T_o)}{a^2 x}$ is the Grashof number, $M^2 = \frac{\sigma_f B_o^2}{\rho_f a}$ is the magnetic field parameter, $R_d = \frac{4\sigma^* T_\infty^3}{k^* k_f}$ is the Radiation parameter, $\Pr = \frac{\mu_f (C_p)_f}{k_f}$ is the Prandtl number, $Q_s = \frac{Q}{(\rho C_p)_f a}$ is the heat source parameter, Here $f_\Omega = \frac{\partial f}{\partial \Omega}, \theta_\Omega = \frac{\partial \theta}{\partial \Omega}$ and so on. $A_3 = (1-(\Phi_1+\Phi_2+\Phi_3)) + \Phi_1\frac{(\rho\beta)_{s1}}{(\rho\beta)_f} + \Phi_2\frac{(\rho\beta)_{s2}}{(\rho\beta)_f} + \Phi_3\frac{(\rho\beta)_{s3}}{(\rho\beta)_f}$ is the Eckert number.

Dimensionless boundary conditions

$$f_\Omega(0)=1,\ f(0)=0\ \ \theta_\Omega(0)=-\frac{B_i}{A_5}(1-\theta(0))$$
$$(11)\ f_\Omega(\infty)=0,\ \theta(\infty)=0$$

where

$B_i=\frac{h_f}{k_f}(\frac{\nu_f}{a})^{\frac{1}{2}}$ is the Biot number.

The terms are derived from the above equations as follows:

$$A_1=(1-(\Phi_1+\Phi_2+\Phi_2))^{2.5}$$

$$A_2=(1-(\Phi_1+\Phi_2+\Phi_3))+\Phi_1\frac{\rho_{s1}}{\rho_f}+\Phi_2\frac{\rho_{s2}}{\rho_f}+\Phi_3\frac{\rho_{s3}}{\rho_f}$$

$$A_3=(1-(\Phi_1+\Phi_2+\Phi_3))+\Phi_1\frac{(\rho\beta)_{s1}}{(\rho\beta)_f}+\Phi_2\frac{(\rho\beta)_{s2}}{(\rho\beta)_f}+\Phi_3\frac{(\rho\beta)_{s3}}{(\rho\beta)_f}$$

$$A_4=(1-(\Phi_1+\Phi_2+\Phi_3))+\Phi_1\frac{(\rho C_p)_{s1}}{(\rho C_p)_f}+\Phi_2\frac{(\rho C_p)_{s2}}{(\rho C_p)_f}+\Phi_3\frac{(\rho C_p)_{s3}}{(\rho C_p)_f}$$

$$A_5=\frac{k_{thnf}}{k_f},A_6=\frac{\sigma_{thnf}}{\sigma_f}$$

The two most important quantities of practical importance in the current inquiry are skin friction and Nusselt number which are given by

Skin friction $(\tau)=\frac{\mathrm{Re}^{\frac{-1}{2}}}{A_1}f_{\Omega\Omega}(\Omega)$

Nusselt number (Nu) $=-A_5\,\mathrm{Re}^{\frac{1}{2}}\theta_\Omega(\Omega)$

Where $\mathrm{Re}=\frac{a^2x}{\nu_f}$ is the Reynolds number.

Numerical procedure

The velocity equation,[9] temperature equation,[10] and the associated boundary conditions[11] are solved numerically using a mathematical software tool, employing the RKF-45 method along with the shooting technique. These equations, being higher-order with two-point

boundary conditions, are converted into a system of first-order initial value problems to facilitate the solution process.

We consider

$$\frac{df}{d\Omega} = f_1, \frac{d^2 f}{d\Omega^2} = \frac{df_1}{d\Omega} = f_2, \frac{d^3 f}{d\Omega^3} = \frac{df_2}{d\Omega} = f_3$$

$$\frac{d\theta}{d\Omega} = g_1, \frac{d^2\theta}{d\Omega^2} = \frac{dg_1}{d\Omega} = g_2$$

$$f_3 - (A_1A_2)[f_1^2 - ff_2] - A_1A_6M^2 f_1 + (A_1A_3)G\theta = 0 \qquad (12)$$

$$A_1[A_5 + \frac{4}{3}R_d]g_2 + A_1A_4P_r fg_1 + A_1P_rQ_s\theta + E_cP_r(f_2)^2 + A_1A_6P_rM^2E_c f_1^2 = 0 \qquad (13)$$

With

$$\left.\begin{aligned} f_1 = 0, f = 0, g_1 = -\frac{B_i}{A_5}(1-\theta) \text{ at } \Omega = 0 \\ f_1 \to 0, \theta \to 0 \text{ as } \Omega \to \infty \end{aligned}\right\} \qquad (14)$$

The transformed initial value problem is solved by estimating the missing values using the shooting method after selecting the appropriate parameters. A step size of 0.1 is used for the calculations, with an error tolerance of approximately 10^{-6}.

Comparison

Table 3: A comparison of the current findings with those of Haritha et al. is made regarding the heat transfer rate for various values of P_r when $R_d = E_c = 0$.

P_r	Manjunatha et al.[36]	Haritha et al.[37]	Present values
2	0.9113	0.9114	0.9112
6.13	1.7596	1.7595	1.7597
20	3.3539	3.3538	3.3534

OUTCOMES & DISCUSSION

The effect of key variables on the velocity and the temperature is illustrated in the figures 2a-2b, 3a-3b, 4a-4b, 5a-5b, 6a-6b, 7a-7b. The parameter values adapted for this investigation include: $\Phi = 0.01, G = 0.2, M = 0.1, R_d = 2.5, Q_s = 0.5, E_c = 0.1, P_r = 6.2, B_i = 0.1$. This work explores how these parameters influence the flow and the temperature profiles inside the ternary nanofluid system under the given conditions.

Fig.(2a) represents the variation of axial velocity (f') with nanoparticle volume fraction Φ. The fluid velocity (f') depreciates when Φ(solid volume fraction) increases in both nanofluids. Enhancement in Φ heightens the fluid boundary layer, lowering the fluid velocity. The magnitude of f' in ternary nanofluid is smaller than that of hybrid nanofluid. Fig.(2b) represents the variation of temperature (θ) with Φ.The fluid temperature upsurges with the higher values of Φ. The thermal conductivity of the nanofluid is a function of the thermal conductivity of both the base fluid and the nanoparticles. Increasing the nanoparticle volume fraction results in the increase in the conductive heat transfer coefficient and consequently the convective heat transfer. Increasing the thermal conductivity leads to the increase in the efficiency of the fluid heat transfer. This agrees with the physical behaviour that, when the volume fraction parameter Φ enhances, the thermal conductivity increases and consequently the thermal boundary layer thickness increases. This may be attributed to the fact that thickness of thermal boundary layer enhances on par with the larger values of Φ. The temperature in ternary nanofluid is greater than that in hybrid nanofluid.

Figs.(3a & 3b) exhibit the impact of G on f' & θ. It is noted that an increment in G leads to the enhancement in the magnitude of f' and depreciation in θ. This can be attributed to the fact that rising G thickens the momentum boundary layer while thermal boundary layer becomes thin in entire flow region.

The impact of magnetic parameter (M) on f' & θ is exhibited in figs. (4a & 4b). It is noted that f' experiences depreciation when M augments. This is due to the fact that the thickness of momentum boundary layer decays when M grows. In case of θ, opposite effect is observed when M increases in both ternary and hybrid nanofluids. This is in accord with the physics of the problem, since the application of transverse magnetic field results in resistive type force (The Lorentz force) similar to the drag force which tends to resist the fluid flow and thus reduces its f' and enhances its θ.

Figs.(5a-5b) exhibit the influence of thermal radiation (R_d) on f', θ. An increasing in R_d results to augmentation in magnitude of $f'$and θ in entire flow region. This may be attributed to the fact that increasing in Rd enhances the thickness of momentum and thermal boundary layers in both nanofluids.

The effect of dissipative energy (E_c) has been observed in figs. (6a & 6b). From the graph we notice that higher E_c larger the velocity (fig.(6a)). This may be due to the fact that the thickness of momentum boundary layer experiences grow for larger values of E_c . A higher E_c indicates that more kinetic energy is converted into internal energy through dissipation. This leads to increased heat generation within the flow. Consequently, temperature profile becomes steeper near the solid boundaries where viscous dissipation is significant, causing the temperature of the fluid to rise (fig. (6b)).

It is identified from the graphs that the values of f' & θ in ternary nanofluid are relatively greater than those in hybrid nanofluid.

Skin friction (τ) increases and Nusselt number (Nu) decreases at the stretching sheet in both ternary as well as hybrid nanofluid with the increasing values of $\Phi / R_d / E_c / Q_s$. In case of M / Bi , both τ and Nu are depreciated in both nanofluids at the stretching sheet while G appreciates τ and Nu. (Table. (4)).

It is noted from the graphs that the values of Nu in ternary nanofluid are relatively greater than those in hybrid nanofluid .

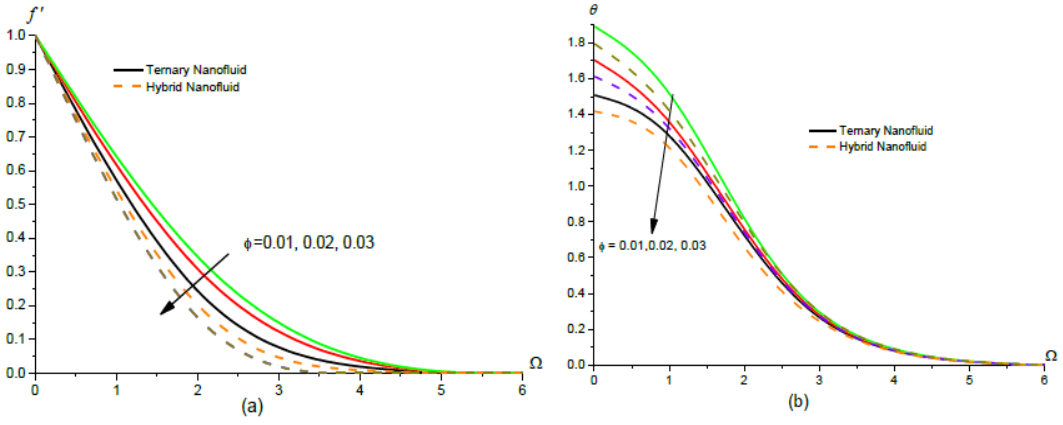

Fig. 2: Effect of Φ on (a) Velocity and (b) Temperature.

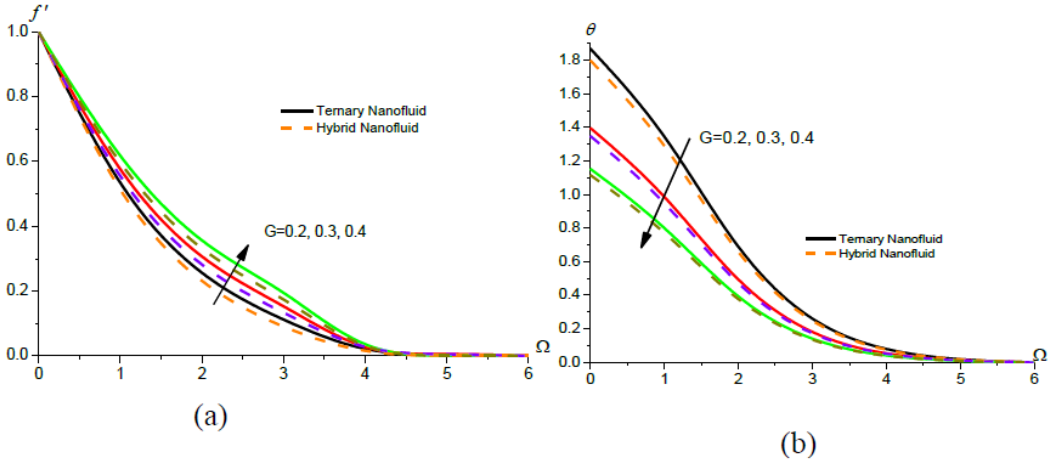

Fig. 3: Effect of G on (a) velocity and (b) temperature.

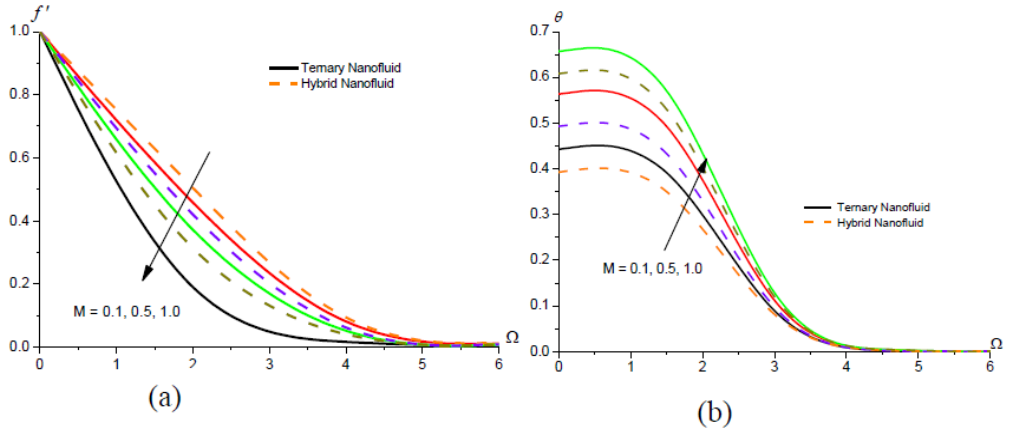

Fig. 4: Effect of M on (a) velocity and (b) temperature.

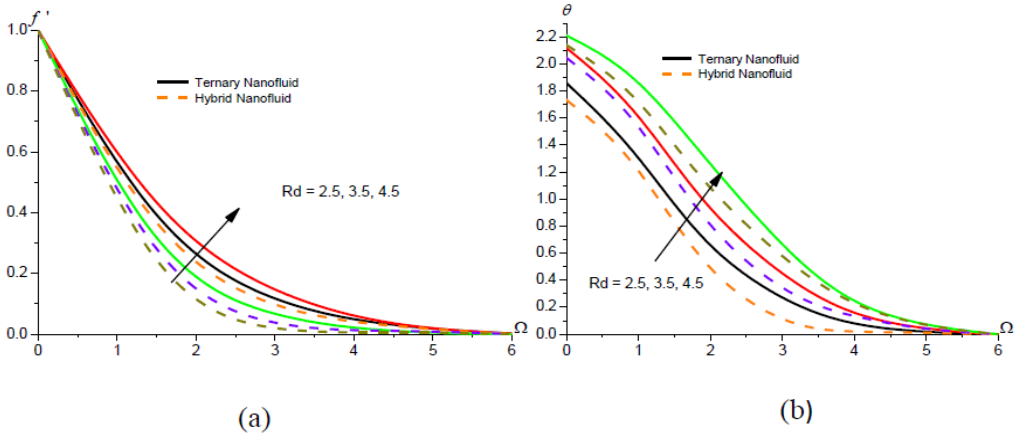

Fig. 5: Effect of R_d on (a) velocity and (b) temperature.

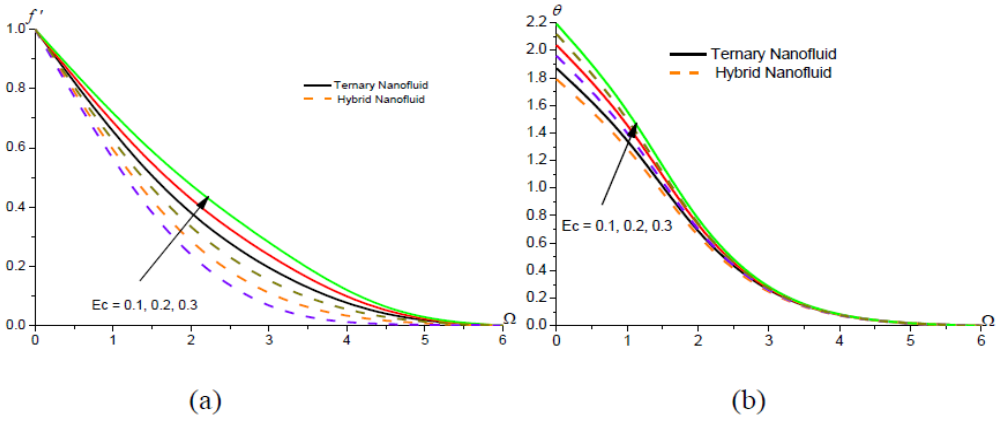

(a) (b)

Fig. 6: Effect of E_c on (a) velocity and (b) temperature.

Table 4: Effects of different parameters on Skin friction (τ) and Nusselt number(Nu) for ternary and hybrid nanofluids at $\Omega = 0$

Parameter	Ternary Nanofluid		Hybrid Nanofluid	
	τ(0)	Nu(0)	τ(0)	Nu(0)
Φ	-0.86882	-0.09757	-0.87987	-0.08979
	-0.85768	-0.10567	-0.87921	-0.10213
	-0.84646	-0.11414	-0.87818	-0.11473
G	-0.82517	-0.09217	-0.83567	-0.08482
	-0.79961	-0.04214	-0.80963	-0.03706
	-0.77624	-0.01627	-0.78585	-0.01232
M	-0.82517	-0.09217	-0.83567	-0.08482
	-0.8537	-0.16771	-0.86632	-0.16102
	-0.92523	-0.41401	-0.94255	-0.41021
Rd	-0.82517	-0.09217	-0.83567	-0.08482
	-0.77146	-0.11868	-0.78116	-0.11109
	-0.74315	-0.12844	-0.75223	-0.12100
Qs	-0.82517	-0.09217	-0.83567	-0.08482
	-0.58882	-0.29700	-0.60158	-0.28141
	-0.28018	-0.59333	-0.29524	-0.56645
Pr	-0.82517	-0.09217	-0.83567	-0.08482
	-0.86222	-0.07094	-0.87283	-0.06409
	-0.89633	-0.04986	-0.90689	-0.04363
Ec	-0.82517	-0.09217	-0.83567	-0.08482
	-0.80446	-0.11011	-0.81467	-0.10247
	-0.78566	-0.12650	-0.79562	-0.11859
Bi	-0.82517	-0.09217	-0.83567	-0.08482
	-0.84734	-0.14127	-0.85653	-0.13029
	-0.86184	-0.17037	-0.87018	-0.15744

CONCLUSION

From this study we conclude that

- f' decays while θ upsurges for higher values of Φ in both ternary and hybrid nanofluids.
- Magnetic parameter (M) decays f' and enhances θ in ternary as well as hybrid nanofluid. Reverse effect is observed in case of G.
- E_c and R_d enhance both velocity and temperature in the entire flow region.
- M / Bi decays rate of heat transfer in ternary and hybrid nanofluids at the stretching sheet G enhances it.

Nomenclature

u, v velocity components in x, y directions

B_o induced magnetic field

τ skin friction

q_r radiative heat flux

Q_s heat source parameter

Nu Nusselt number

Pr Prandtle number

Cp specific heat at constant preassure

M Magnetic field parameter

T temperature of the fluid

Tw temperature of the wall

$T\infty$ ambient temperature

σ^* Stefan-Boltzmann constant

σ electrical conductivity of the fluid

ρ density of the fluid

Φ_1 solid volume fraction of copper particles

Φ_2 solid volume fraction of iron oxide particles

Φ_3 solid volume fraction of silicon dioxide particles

f fluid

nf nanofluid

hnf hybrid nanofluid

$thnf$ ternary hybrid nanofluid

REFERENCES

1. Choi S. U. S and Eastman, A: Enhancinh thermal conductivity of fluids with Nanoparticles, ASME publications, 1995; 231: 99-106.[1]
2. Buongiorne, J: Convective transport in Nanofluids, Journal Heat transfer, 2006; 128: 250-250.[2]
3. Eastman, J. A., S. U. S Choi, S, Li, W. Yu, and J. Thomson: Anomalously increased effective thermal conductivities of Ethylene Glycol based Naqnofluids containing Copper nanoparticles, Applications Physical Letters, V, 2001; 78: 718-720.[3]
4. Sheikholeslami M, Ganji DD, Javed MY, Ellahi R. Effect of thermal radiation on magneto-hydrodynamics nanofluid flow and heat transfer by means of two phase model. J Magn Magn Mater, 2015; 374: 36–43.[4]
5. Yin, C, L. Zheng, C. Zhang, and X. Zhang: Flow and Heat transfer of Nanofluids over a rotating Disk with uniform stretching rate in the radial direction, Propeller Power Research, V, 2017; 6: 25-30.[5]
6. Zhang, C, L. Zheng, X. hang and C. Chen: MHD flow and radiation heat transfer of nanofluids in poprous media with variable surface heat flux and chemical reaction, Applications Mathematical Modern, V, 2015; 39: 165-1821.[6]
7. Jana, S.; Khojin, A. S.; Zhong, W. H. Enhancement of fluid thermal conductivity by the addition of single and hybrid nano-additives. Thermochimica, 2007; 462: 45–55. [CrossRef][7]
8. Suresh, S.; Venkitaraj, K.P.; Selvakumar, P. Synthesis, characterization of Al2O3-Cu nanocomposite powder and water based nanofluids. Adv. Mater. Res, 2011; 328: 1560–1567. [CrossRef][8]
9. Izady, M.; Dinarvand, S.; Pop, I.; Chamkha, A. Flow of aqueous Fe2O3-CuO hybrid nanofluid over a permeable stretching/ shrinking wedge: A development on Falkner-Skan problem. Chin. J. Phys, 2021; 74: 406–420. [CrossRef][9]
10. Rajesh, V.; Sheremet, M. A.; Öztop, H. F. Impact of hybrid nanofluids on MHD flow and heat transfer near a vertical plate with ramped wall temperature. Case Stud. Therm. Eng, 2021; 28: 101557. [CrossRef][10]
11. Khan, S. A.; Hayat, T.; Alsaedi, A. Irreversibility analysis for nanofluid (NiZnFe2O4-C8H18 and MnZnFe2O4-C8H18) flow with radiation effect. Appl. Math. Comput, 2022; 419: 126879. [CrossRef][11]
12. Qomi, M. E.; Sheikhzadeh, G. A.; Fattahi, A. On the micro-scale battery cooling with a sinusoidal hybrid nanofluid flow. J. Energy Storage, 2021; 46: 103819. [CrossRef][12]

13. Rauf, A.; Shah, N. A.; Mushtaq, A.; Botmart, T. Heat transport and magnetohydrodynamic hybrid micropolar ferrofluid flow over a non-linearly stretching sheet. AIMS Math, 2023; 8: 164–193. [CrossRef][13]
14. Ajeena, A. M.; Víg, P.; Farkas, I. A comprehensive analysis of nanofluids and their practical applications for flat plate solar collectors: Fundamentals, thermophysical properties, stability, and difficulties. Energy Rep, 2022; 8: 4461–4490. [CrossRef][14]
15. Ramesh, G.; Madhukesh, J.; Shah, N. A.; Yook, S.-J. Flow of hybrid CNTs past a rotating sphere subjected to thermal radiation and thermophoretic particle deposition. Alex. Eng. J, 2023; 64: 969–979. [CrossRef][15]
16. Qureshi, M. Z. A.; Faisal, M.; Raza, Q.; Ali, B.; Botmart, T.; Shah, N. A. Morphological nanolayer impact on hybrid nanofluids flow due to dispersion of polymer/CNT matrix nanocomposite material. AIMS Math, 2023; 8: 633–656. [CrossRef][16]
17. Bhatti, M.; Öztop, H.F.; Ellahi, R.; Sarris, I.E.; Doranehgard, M. Insight into the investigation of diamond (C) and Silica (SiO2) nanoparticles suspended in water-based hybrid nanofluid with application in solar collector. J. Mol. Liq, 2022; 357: 119134. [CrossRef][17]
18. Venkateswarlu B, Satya Narayana P.V. $Cu-Al_2O_3/H_2O$ hybrid nanofluid flow fast a porous stretching sheet due to temperature dependent viscosity and viscous dissipation. Heat transfer, 2020; 1-18. https://doi.org/10.1002/htj.21884.[18]
19. Malleswari Kakanti, Kata Sreelakshmi, Ganganapalli Sarojamma & Ali J. Chamka, 2022: Effect of stratification and non-linear radiant energy on MHD unsteady flow of $Ag-Al_2O_3/C_2H_6O_2$-water on an elongated surface, Inernational Journal of Ambient Energy, DOI: 10.1080/01430750.2022.2029766.[19]
20. Hayat T, Nadeem S. Heat transfer enhancement with $Ag-CuO/H_2O$ hybrid nanofluid. Results Phys, 2017; 7: 2317-2324.[20]
21. Mousavi, S.M.; Esmaeilzadeh, F.; Wang, X.P. Effect of temperature and particles volume concentration on the thermophysical properties and the rheological behaviour of $CuO/TiO_2/MgO$ aqueous ternary hybrid nanofluid. J. Therm. Anal. Calorim, 2019; 137: 879-901.[21]
22. Sahoo, R.R.; Kumar, V. Development of a new correlation to determine the viscosity of ternary hybrid nanofluid. Int. Commun. Heat Mass Transf, 2019; 111: 104451. [CrossRef][22]

23. Guedri, K.; Khan, A.; Gul, T.; Mukhtar, S.; Alghamdi, W.; Yassen, M.F.; Eldin, E.T. Thermally Dissipative Flow and Entropy Analysis for Electromagnetic Trihybrid Nanofluid Flow Past a Stretching Surface. ACS Omega, 2022; 7: 33432–33442. [CrossRef][23]
24. Xuan, Z.; Zhai, Y.; Ma, M.; Li, Y.; Wang, H. Thermo-economic performance and sensitivity analysis of ternary hybrid nanofluids. J. Mol. Liq, 2020; 323: 114889. [CrossRef][24]
25. Algehyne, E.A.; Alrihieli, H.F.; Bilal, M.; Saeed, A.;Weera,W. Numerical approach toward ternary hybrid nanofluid flow using variable diffusion and non-Fourier's concept. ACS Omega, 2022; 7: 29380–29390. [CrossRef][25]
26. Ramesh GK, Madhukesh JK. Shehzab SA, Rauf A. Ternary nanofluid with heat source/sink and porous medium effects in stretchable convergent/divergent channel. Proceedings of the institution of Mechanical Engineers, Part E: Journal of Process Mechanical Engineering, 2024; 238(1): 134-143.doi:10.1177/09544089221081344.[26]
27. Kumar, S.S.; Prasad, R.V.; Kumar, M.S.; Mamatha, S.U.; Raju, C.S.K.; Raju, K.V.B. Dynamical nonlinear moments of internal heating impact on hydro-magnetic flow suspended with pure water-based CNT+Graphene+Al2O3 and Paraffin wax+Sand+AA7072 mixtures. Int. J. Mod. Phys. B, 2022; 37: 2350150. [CrossRef][27]
28. Jafar Hasnain & Nomana Abid (2023) Numerical investigation for thermal growth in water and engine oil-based ternary nanofluid using three different shaped nanoparticles over a linear and nonlinear stretching sheet, Numerical Heat Transfer, Part A: Applications, 2023; 83, 12: 1365-1376, DOI: 10.1080/10407782.2022.2104582.[28]
29. W. Ashraf Adnan, Thermal efficiency in hybrid ($Al_2O_3 - CuO/H_2O$) and ternary hybrid nanofluids ($Al_2O_3 - CuO - Cu/H_2O$) by considering novel effects of imposed magnetic field and convective heat condition, in: Waves in Random and Complex Media, 2022, https://doi.org/10.1080/17455030.2092233.[29]
30. Kamel Guedri, Arshad Khan, Ndilane Sene, Zehba Raizah, Anwar Saeed, Ahmed M. Galal, "Thermal flow of Radiative Ternary Hybrid Nanofluid over Nonlinear stretching sheet Subject to Darcy-Forchheimer Phenomenon", Mathematical Problems in Engneering, 2022, Article ID 3429439, 2022; 14. https://doi.org/10.1155/2022/3429439.[30]

31. Vishalakshi, A. B.; Mahabaleswar U.S.; Laroze, D; Zeidan, D. "A study of mixed convective ternary hybrid nanofluid flow over a stretching sheet with radiation and transpiration", Special topics and reviews in porous.
32. Sharma, R.P. Badak, K. Heat transport of radiative ternary hybrid nanofluid over a convective stretching sheet with induced magnetic field and heat source/sink. J Therm Anal Calorim, 2024. https://doi.org/10.1007/s10973-024-12979-y.[32]
33. Aly EH, Pop I. MHD flow and heat transfer neat stagnation point over a stretching/shrinking surface with partial slip and viscous dissipation: Hybrid nanofluid versus nanofluid. *Power Technol,* 2020; 367: 192-205.[33]
34. Lund LA, Omar Z, Khan I, Seikh AH, Nisar KS. Stability analysis and multiple solutionof Cu-Al_2O_3/H_2Onanofluid contains hybrid nanomaterials over a shrinking surface in the presence of viscous dissipation. *J Mater Res Technol,* 2020; 9(1): 421-432.[34]
35. Afridi MI, Quasim M, Khan NA, Hamdani M. Heat transfer analysis of Cu-Al_2O_3-water and Cu-Al_2O_3-kerosene oil hybrid nanofluids in the presence of frictional heating: Using 3-state Lobatto IIIa formula. *J Nanofluid,* 2019; 8(4): 885-891.[35]
36. Manjunatha S., Puneeth V., Gireesha B.J., Chamka, A. J. Theoretical study of convective heat transfer in ternary nanofluid flowing past a stretching sheet, J. Appl. Comput. Mech, 2022; 8(4): 1279-1286. https://doi.org/10.22055/JACM.2021.37698.3067[36]
37. Haritha, A., Devasena, Y., Rohit Royal, D. Analysis of heat transfer in ternary hybrid nanofluids over a stretching sheet with radiation and heat source using Machine Learning Algorithm. Stochastic Modelling and Computational Sciences, ISSN:2752-3829, 2023; 3: 2.[37]